# Nonlinear Control of Two-Wheeled Robot Based on Novel Analysis and Design of SDRE Scheme

Li-Gang Lin, *Member, IEEE*, and Ming Xin, *Senior Member, IEEE*

***Abstract*— This brief presents a nonlinear control design for a two-wheeled inverted pendulum robot, based on new analysis of the classical state-dependent Riccati equation (SDRE) scheme and a novel alternative strategy. The solvability of pointwise algebraic Riccati equations (AREs) corresponding to the nonunique state-dependent coefficients (SDCs) of the SDRE scheme is analyzed from a new perspective. This is formulated as a simple equivalence condition with reduced dimensionality, which circumvents the excessive online computational effort to check the solvability of classical SDRE. The condition is derived in a way to facilitate the generalization to all meaningful SDCs. Moreover, due to unsolvable AREs, all conflicts against the primary objective of posture balance of the robot are revealed and illustrated, with a connection to the robot physical parameters. At the system states that cause such conflicts and other unsolvable AREs, a simple analytical solution via alternative SDC constructions is suggested. More potential advantages of this SDC construction over the classical scheme are revealed in simulations, e.g., the maximum input/torque and total energy consumption.**

***Index Terms*— Applicability and computational analysis, nonlinear control systems, state-dependent Riccati equation (SDRE), wheeled inverted pendulum (WIP).**

## I. Introduction

In RECENT years, the research on two-wheeled mobile robots, or wheeled inverted pendulum (WIP), has attracted tremendous attention among the robotics/control community. A recent survey [1] summarized various advantages of WIP, e.g., high maneuverability/agility without tipping over and to traverse rough terrain. The successful commercialized product, *Segway* and its variants, also explains its popularity. However, as intuitively anticipated, the balancing of WIP has been the primary control objective, which truly challenges many existing design strategies. Among various control designs addressing this issue, a large portion is based on the linear (state-feedback) control due to its well-established theory. In particular, the design via linear quadratic regulator (LQR) gains its wide popularity because of the optimality guarantees with respect to the linearized dynamics, which has been validated by real-time implementations [1]. As a step forward, more focus is gradually set on the nonlinear control systems of WIP. This trend can be partially explained by:

i) the effect of the nonlinear dynamics is too prevailing to be neglected/linearized, in the presence of, e.g., fast yaw rotation, large pitch deviation, and abrupt start/stop [2] and

ii) the WIP system is underactuated, restricted by nonholonomic motion constraints and, consequently, cannot be smoothly stabilized [3]. To address these challenges, various nonlinear control techniques have been applied with pros and cons, such as those designs reported in [1], [4], and [5], and, more recently, the state-dependent Riccati equation (SDRE) scheme [2].

The growing literature on the SDRE scheme is attributed to its many distinct advantages [6], [7]. For example, this nonlinear optimal control technique: 1) naturally extends from the renowned LQR design (including the finite-time capability [8]); 2) preserves all the essential system nonlinearities; 3) bears flexibilities of nonunique state-dependent coefficients (SDCs) [9] and state/control weighting functions; 4) exhibits robustness against disturbances/uncertainties due to the pointwise/state-dependent nature [10]; and 5) guarantees the global asymptotic stability under certain conditions [11]. Note that, regarding 2), the scheme precludes any truncation/linearization/assumption of (nonlinear) system dynamics. Regarding 3), these flexibilities are additional design degrees of freedom to improve the overall system performance. However, it is reported that the practical achievements have outpaced the theoretical developments [6]. For example, the above-mentioned SDC flexibility is usually implemented following an empirical guideline, but the associated feasibility, i.e., solvability of the corresponding SDRE, is either assumed or resorted to online computing capability [6]. The latter, nonetheless, accounts for a significant implementation burden. Hence, this brief is motivated to theoretically resolve such an issue for the considered robotic system. This new strategy can be readily extended to more applications.

Regarding the SDRE-controlled WIP systems, this brief is pioneered by Kim and Kwon [2]. In their work, the critical issue in the early SDRE design stage is addressed, i.e., how to construct appropriate SDCs, particularly from a modeling perspective. Based on insight into the WIP dynamics, this model-based control design establishes several connections between the specific elements in an SDC and the system response (e.g., high-gain effect), which are experimentally validated. In addition, the primary control objective to keep the inherently unstable pitch motion balanced is achieved and also demonstrated through experiments. Notably, various (non)linear control strategies have been tried but not preferred. Therefore, a reported shortage in most WIP control systems,

Manuscript received November 9, 2018; accepted February 8, 2019. Date of publication March 11, 2019; date of current version April 13, 2020. Manuscript received in final form February 12, 2019. This work was supported in part by Max Planck Society, Germany, and in part by the Ministry of Science and Technology, Taiwan, under Grant 105-2917-I-564-045. Recommended by Associate Editor A. Pavlov. *(Corresponding author: Ming Xin.)*

L.-G. Lin is with the Max Planck Institute for Dynamics of Complex Technical Systems, 39106 Magdeburg, Germany (e-mail: linl@mpi-magdeburg.mpg.de).

M. Xin is with the Department of Mechanical and Aerospace Engineering, University of Missouri, Columbia, MO 65211 USA (e-mail: xin@missouri.edu).

Color versions of one or more of the figures in this article are available online at http://ieeexplore.ieee.org.

Digital Object Identifier 10.1109/TCST.2019.2899802

for comparing different design strategies [1], is filled in [2]. However, in this brief, a pitfall of unsolvable SDREs is revealed when the design framework is analyzed from a computational perspective, which motivates this brief to provide further support.

The problem of SDRE-based nonlinear optimal control for WIP is formulated in a generalized coordinate frame, given the dynamics in [2]. The main contributions of this brief are as follows.

1) Following the classical SDRE scheme [6], all the SDC matrices with modeling benefits [2] are analyzed from a computational perspective. The solvability of the corresponding algebraic Riccati equation (ARE) is analytically *unified* as one compact equivalence condition, in a reduced-dimensional state space. Therefore, the traditional online computational burden in examining the pointwise solvability of AREs is avoided.
2) Considering the primary objective to balance the WIP's pitch motion, all the conflicts against this objective due to unsolvable AREs are revealed, and the associated geometry is clearly illustrated. This provides engineers valuable insights into the configuration design of pendulum body moment of inertias (MOIs).
3) At those system states of unsolvable AREs, including those conflicts in 2), an alternative simple analytical solution (Alternative SDRE) is suggested. Its various potentials leading to performance advantages are revealed in simulations.

## II. SDRE Overview and WIP Dynamics Formulation

### A. Outline of SDRE Scheme

Consider the nonlinear, autonomous, and control-affine systems, with a quadratic-like performance index as follows:

$$\dot{\mathbf{x}} = \mathbf{f}(\mathbf{x}) + B(\mathbf{x})\mathbf{u} \tag{1}$$

$$J = \frac{1}{2}\int_0^\infty \{\mathbf{x}^T Q(\mathbf{x})\mathbf{x} + \mathbf{u}^T R(\mathbf{x})\mathbf{u}\}dt \tag{2}$$

where $\mathbf{x} \in \mathbb{R}^n$, $\mathbf{u} \in \mathbb{R}^m$, and the functions $\mathbf{f}(\mathbf{x})$, $B(\mathbf{x}) \neq 0$, $Q(\mathbf{x}) = Q^T(\mathbf{x}) \geq 0$, and $R(\mathbf{x}) = R^T(\mathbf{x}) > 0$ pointwise are of compatible dimensions and continuously differentiable. Conceptually, the SDRE scheme is a *pointwise* nonlinear extension of the LQR design, by treating the system parameters as if they were frozen/constant at each instant [6]. The following general procedure shares similarities to the LQR.

1) Factorize $\mathbf{f}(\mathbf{x}) = A(\mathbf{x}) \cdot \mathbf{x}$, where $A(\mathbf{x}) : \mathbb{R}^n \to \mathbb{R}^{n\times n}$ is the nonunique SDC matrix (a design flexibility).
2) Solve the SDRE in the following equation for its solution $P(\mathbf{x}) : \mathbb{R}^n \to \mathbb{R}^{n\times n}$:

$$A^T(\mathbf{x})P(\mathbf{x}) + P(\mathbf{x})A(\mathbf{x}) + Q(\mathbf{x}) - P(\mathbf{x})B(\mathbf{x})R^{-1}(\mathbf{x})B^T(\mathbf{x})P(\mathbf{x}) = 0. \tag{3}$$

3) The SDRE controller is $\mathbf{u}(\mathbf{x}) = -R^{-1}(\mathbf{x})B^T(\mathbf{x})P(\mathbf{x})\mathbf{x}$.

Unless otherwise mentioned, we denote for brevity $\mathbf{f} = \mathbf{f}(\mathbf{x})$, $A = A(\mathbf{x})$, $B = B(\mathbf{x})$, $Q = Q(\mathbf{x})$, $R = R(\mathbf{x})$, $P = P(\mathbf{x})$, and $C := C(\mathbf{x}) = Q^{1/2}$ is a full-rank matrix. Moreover, we follow the notations of SDC matrix sets [12]: $\mathcal{A}_{\mathbf{xf}}$, $\mathcal{A}^c$, $\mathcal{A}^s$, $\mathcal{A}^o$, $\mathcal{A}^d$, $\mathcal{A}^l$, and $\mathcal{A}^i$ as the sets of $A$ such that $A \cdot \mathbf{x} = \mathbf{f}$, $(A, B)$ is controllable, $(A, B)$ is stabilizable, $(A, C)$ is observable, $(A, C)$ is detectable, $(A, C)$ has no unobservable mode on the closed left half-plane, and $(A, C)$ has no unobservable mode on the imaginary axis, respectively; $\mathcal{A}_{\mathbf{xf}}^{si} = \mathcal{A}_{\mathbf{xf}} \cap \mathcal{A}^s \cap \mathcal{A}^i$ and similar to others. Finally, denote $\mathcal{N}(\cdot)$, $\mathcal{R}(\cdot)$, $||\cdot||$, $\lambda(\cdot)$, $\mathbb{R}_{>0}$ and $\mathbb{R}_{<0}$ as the null space, range space, $l_2$ norm, spectrum/eigenvalues of a matrix/vector, set of positive real numbers, and set of negative real numbers, respectively.

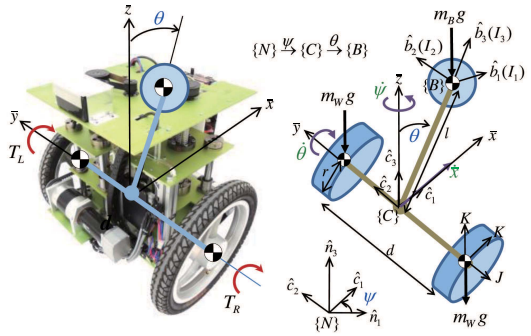


Fig. 1. Schematic of two-wheeled robot [2].

Analytically, the applicability of SDRE scheme, i.e., pointwise solvability of SDRE (3) at any nonzero state, is summarized in Lemma 1 as follows. Accordingly, any SDC matrix residing in the nonempty set, $\mathcal{A}_{\mathbf{xf}}^{si}$ or $\mathcal{A}_{\mathbf{xf}}^{sl}$, is called *feasible*.

*Lemma 1 [12], [13]:* At any state $\mathbf{x} \in \mathbb{R}^n\backslash\mathbf{0}$ of system (1). The following three statements are pointwise equivalent.

1) SDRE (3) admits the unique and Hurwitz $P = P^T \geq 0$.
2) $\mathcal{A}_{\mathbf{xf}}^{si} = \mathcal{A}_{\mathbf{xf}} \cap \mathcal{A}^s \cap \mathcal{A}^i \neq \emptyset$, i.e., there exists an SDC matrix $A$ such that $A \cdot \mathbf{x} = \mathbf{f}$, $(A, B)$ is stabilizable, and $(A, C)$ has no unobservable mode on the imaginary axis.
3) $C\mathbf{x} \neq \mathbf{0}$ or $\mathbf{f} \neq \mathbf{0}$.

Similarly, the counterpart for $P > 0$ is: i) SDRE (3) admits the unique, symmetric, and Hurwitz $P > 0$; ii) $\mathcal{A}_{\mathbf{xf}}^{sl} = \mathcal{A}_{\mathbf{xf}} \cap \mathcal{A}^s \cap \mathcal{A}^l \neq \emptyset$; and iii) $C\mathbf{x} \neq \mathbf{0}$ or $\mathbf{f} \neq \mu\mathbf{x}$, for some $\mu \leq 0$.

### B. WIP Dynamic Systems Formulation

A recent model is adopted from [2], with its schematic illustrated in Fig. 1. The modeling procedure is based on several preliminary results, e.g., [25] and [26], where rigorous comparisons with respect to other modeling approaches are also investigated. In terms of the generalized coordinate frame, denote $(\bar{x}, \theta, \psi)$ as the straight-ahead movement [m], pitch, and yaw angles [rad] of WIP, and $(T_L,\ T_R)$ as the left and right wheel torques [N·m], respectively. The nonlinear dynamics of motion are [2]

$$\begin{aligned}
\eta_1\ddot{\bar{x}} &= m_B l \mathrm{s}\theta\{\dot{\psi}^2[I_2 + m_B l^2 + (I_3 - I_1 - m_B l^2)\mathrm{c}^2\theta] \\
&\quad - m_B l g \mathrm{c}\theta + (I_2 + m_B l^2)\dot{\theta}^2\} + (T_L + T_R) \\
&\quad \times [m_B l \mathrm{c}\theta + (I_2 + m_B l^2)/r] \\
\eta_1\ddot{\theta} &= \mathrm{s}\theta\{\dot{\psi}^2\mathrm{c}\theta[(I_1 + m_B l^2 - I_3) \\
&\quad \times (m_B + 2m_W + 2J/r^2) - m_B^2 l^2] \\
&\quad + m_B l[g(m_B + 2m_W + 2J/r^2) - m_B l\dot{\theta}^2\mathrm{c}\theta]\} \\
&\quad + (T_L + T_R)[m_B(1 + l\mathrm{c}\theta/r) + 2(m_W + J/r^2)] \\
\eta_2\ddot{\psi} &= \{\dot{\psi}\mathrm{s}\theta[2(I_3 - I_1 - m_B l^2)\dot{\theta}\mathrm{c}\theta - m_B l\dot{\bar{x}}] \\
&\quad + d(T_R - T_L)/r\}
\end{aligned} \tag{4}$$

where $m_B = 45$ (respectively $m_W = 2$) [kg] is the mass of pendulum body (respectively wheel), $l = 0.135$ [m] length of pendulum, $\{I_i\}_{i=1,2,3}$ [kg·m$^2$] MOIs of pendulum body, $g = 9.8$ [m/s$^2$] gravitational constant, $r = 0.2$ [m] radius of wheel, $d = 0.6$ [m] distance between wheels, both $K = 0.04$ and $J = 0.02$ [kg·m$^2$] MOIs of wheel, $\eta_1 := \eta_1(\theta) = m_B(m_B l^2 \mathrm{s}^2\theta + I_2) + 2(m_W + J/r^2)(I_2 + m_B l^2) > 0$, $\eta_2 := \eta_2(\theta) = I_3 + 2[K + (m_W + J/r^2)d^2] + (I_1 + m_B l^2 - I_3)\mathrm{s}^2\theta > 0$, $\mathrm{s}\theta := \sin(\theta)$, and $\mathrm{c}\theta := \cos(\theta)$. To conform to the form of system (1) via the SDRE scheme, let $\mathbf{x} = [\bar{x}, \theta, \psi, \dot{\bar{x}}, \dot{\theta}, \dot{\psi}]^T \in \mathbb{R}^6$, $\mathbf{u} = [T_L, T_R]^T \in \mathbb{R}^2$, and rewrite (4) into the state-space representation as

$$\mathbf{f} = [\, x_4,\ x_5,\ x_6,\ x_2 a_2,\ x_2 a_4,\ x_2 a_6]^T \in \mathbb{R}^6 \tag{5}$$

$$B^T = \left[\begin{array}{c:c:c:c} 0_{2\times 3} & \begin{matrix} b_2 \\ b_2 \end{matrix} & \begin{matrix} b_4 \\ b_4 \end{matrix} & \begin{matrix} b_6 \\ -b_6 \end{matrix} \end{array}\right] \in \mathbb{R}^{2\times 6} \tag{6}$$

where $a_2(x) = \mathrm{s}x_2\{m_B l[I_2 + m_B l^2 + (I_3 - I_1 - m_B l^2)\mathrm{c}^2 x_2]x_6^2 - m_B^2 l^2 g \mathrm{c}x_2 + (I_2 + m_B l^2)m_B l x_5^2\}/(x_2\eta_1)$, $a_4(x) = \{[(I_1 + m_B l^2 - I_3)(m_B + 2m_W + 2J/r^2) - m_B^2 l^2]x_6^2 \mathrm{c}x_2 - m_B^2 l^2 x_5^2 \mathrm{c}x_2 + (m_B + 2m_W + 2J/r^2)m_B l g\}\mathrm{s}x_2/(\eta_1 x_2)$, $a_6(x) = \mathrm{s}x_2[2(I_3 - I_1 - m_B l^2)x_5 x_6 \mathrm{c}x_2 - m_B l x_4 x_6]/(\eta_2 x_2)$; $b_2(x_2) = [m_B l \mathrm{c}x_2 + (I_2 + m_B l^2)/r]/\eta_1$, $b_4(x_2) = -[m_B + 2m_W + 2J/r^2 + (m_B l \mathrm{c}x_2)/r]/\eta_1$, $b_6(x_2) = -d/(r\eta_2)$, as adopted from [2] for easy comparison. Note that this specific representation of (5) and (6) will facilitate the compact formulation of the results in Section III. In addition, $B$ is of full rank, since $b_i \neq 0$, $i = 2, 4, 6$, and B(5:6,:) is invertible for all system states.

## III. Balancing Control Design

The primary objective is to design an SDRE control, such that the WIP robot remains balanced all the time [1]. In this brief, the feasibility of SDC as well as the computational improvement of SDRE scheme constitutes the main focus. Note that the main computational efforts in the SDRE implementation are, pointwise: 1) feasible SDC constructions and verifications and 2) solving the ARE. Given that mature algorithms for 2) already exist, the following two sections provide algebraic/geometric analysis on 1), aiming at a more agile, lower cost, and thus more competitive robotic product. In a general context, this also responds to an expectation toward the computational improvement of SDRE scheme [14].

### A. Solvability/Applicability of Classical SDRE

The critical and challenging design issue in the SDRE scheme is how to implement the flexibility of infinitely many SDCs, i.e., how to construct feasible SDCs [2], [6]. A recent survey [6] summarizes the general principle of classical SDC selections, denoted as *Classical SDRE*, which has been shown effective in many real applications. Regarding the considered WIP control, a recent contribution [2] investigates this issue via *Classical SDRE* from a modeling perspective and clarifies connections between SDC elements and the corresponding system responses.

First, the following SDC matrix in $\mathbb{R}^{6\times 6}$ [2] is considered:

$$A(1:3, 4:6) = I_3 \text{ and } A(4:6, 2) = [a_2, a_4, a_6]^T \tag{7}$$

where $\{a_i\}_{i=2,4,6}$ are given in (5), and the other entries are zero. Because of this SDC formulation (7), possible distortion/undershoot in the pitch trajectory is dominated by the high gain effect of $A(6, :)$ [2]. This is illustrated through simulations and experiments. More nonlinear characteristics of WIP reflected by such an SDC (7) are also investigated therein. As a critical step forward, from a computational perspective, the poinwise solvability of the corresponding AREs with respect to the SDC (7) is analyzed as follows.

Without loss of generality, the following analysis focuses on the popular case of $Q = C^T C > 0$, which implies: 1) $C$ is invertible; 2) $(A, C)$ is observable according to the Popov–Belevitch–Hautus (PBH) test [13]; and 3) $\mathcal{A}_{\mathbf{xf}} = \mathcal{A}_{\mathbf{xf}}^{\beta}$, $\beta = o, d, l, i$. Hence, with respect to the SDC matrix $A$ in (7) and $B$ in (6), it only remains to analyze the stabilizability, i.e., whether $A \in \mathcal{A}_{\mathbf{xf}}^{s}$. Note that the other case of $Q \geq 0$ can be derived similarly [12]. To proceed with the solvability analysis, the preliminaries in Lemma 2 in the following are first recalled, which facilitates the dimension reductions (DRs) in the following main results of this section.

*Lemma 2 [15]:* Let $\Gamma \in \mathbb{R}^{n\times n}$ and $\Pi^T = [\, 0 \,\vdots\, \Pi_2\,] \in \mathbb{R}^{p\times n}$, where $p < n$ and $\Pi_2 \in \mathbb{R}^{p\times p}$ is invertible. Then, $(\Gamma, \Pi)$ is controllable (respectively stabilizable) if and only if (iff) $(\Gamma_{11}, \Gamma_{12})$ is controllable (respectively stabilizable), where $\Gamma_{11} = \Gamma(1 : n-p, 1 : n-p)$ and $\Gamma_{12} = \Gamma(1 : n-p, n-p+1 : n)$. In particular, when $\Gamma_{12} = 0$, then $(\Gamma, \Pi)$ is uncontrollable, and it is stabilizable iff $\mathrm{Re}\{\lambda(\Gamma_{11})\} \subset \mathbb{R}_{<0}$.

*Theorem 1:* Given $Q > 0$, $A$ and $B$ in (6) and (7). The following statements, pointwise at any nonzero system state, are equivalent: 1) SDRE (3) is unsolvable; 2) $A \notin \mathcal{A}_{\mathbf{xf}}^{s\beta}$, $\beta = l, i$; and 3) $\Gamma = 0$, where $\Gamma := \Gamma(\mathbf{x}) = a_2 b_4 - a_4 b_2$, and $\{a_i, b_i\}_{i=2,4}$ are given in (5) and (6).

*Proof:* Given $Q > 0$, we know that: 1) $C$ is also positive definite and invertible; 2) $\mathcal{A}_{\mathbf{xf}}^{s\beta} \neq \emptyset$, $\beta = l, i$, according to Lemma 1; and 3) $\mathcal{A}^o \equiv \mathbb{R}^{6\times 6}$ by the PBH test [15]. Since $\mathcal{A}^o \subseteq \mathcal{A}^l \subseteq \mathcal{A}^i$ [13], from 3), we also have $\mathcal{A}^l \equiv \mathcal{A}^i \equiv \mathbb{R}^{6\times 6}$. Therefore, $\mathcal{A}_{\mathbf{xf}}^{s\beta} = \mathcal{A}_{\mathbf{xf}} \cap \mathcal{A}^s \cap \mathcal{A}^\beta = \mathcal{A}_{\mathbf{xf}} \cap \mathcal{A}^s \cap \mathbb{R}^{6\times 6} = \mathcal{A}_{\mathbf{xf}} \cap \mathcal{A}^s = \mathcal{A}_{\mathbf{xf}}^s$, $\beta = l, i$, and according to Lemma 1, it only remains to analyze $\mathcal{A}_{\mathbf{xf}}^s$ (and the associated $\mathcal{A}_{\mathbf{xf}}^c$).

Considering $A$ in (7) and $B$ in (6), the associated controllability/stabilizability is invariant under any equivalence transformation (ET) [15]. Since $B$ in (6) is of full rank, there exists an ET such that the pair $(A, B)$ can be transformed into the applicable form of Lemma 2, which is able to reduce the dimension of controllability/stabilizability analysis. Specifically, let $(A^{(1)}, B^{(1)}) = (M_B^T A M_B, M_B^T B) \in \mathbb{R}^{6\times 6} \times \mathbb{R}^{6\times 2}$ in the equivalently transformed coordinate, where $M_B \in \mathbb{R}^{6\times 6}$

$$M_B = \left[\begin{array}{c:ccc} I_3 & \multicolumn{3}{c}{0_3} \\ \hdashline 0_3 & \begin{matrix} b_4/\sqrt{b_2^2+b_4^2} \\ -b_2/\sqrt{b_2^2+b_4^2} \\ 0 \end{matrix} & \begin{matrix} 0 \\ 0 \\ 1 \end{matrix} & \begin{matrix} b_2/\sqrt{b_2^2+b_4^2} \\ b_4/\sqrt{b_2^2+b_4^2} \\ 0 \end{matrix} \end{array}\right] \tag{8}$$

$$A^{(1)}(1:3,:)=\left[\begin{array}{c:ccc} 0_3 & \begin{matrix} b_4/\sqrt{b_2^2+b_4^2} & 0 & b_2/\sqrt{b_2^2+b_4^2} \\ -b_2/\sqrt{b_2^2+b_4^2} & 0 & b_4/\sqrt{b_2^2+b_4^2} \end{matrix} \\ & \begin{matrix} 0 & 1 & 0 \end{matrix} \end{array}\right]$$

$$A^{(1)}(4,:)=\left[\begin{array}{cccccc} 0, & \Gamma/\sqrt{b_2^2+b_4^2}, & 0, & 0, & 0, & 0 \end{array}\right] \quad (9)$$

$$(B^{(1)})^T=\left[\begin{array}{c:cc} 0_{2\times 4} & \begin{matrix} b_6 & \sqrt{b_2^2+b_4^2} \\ -b_6 & \sqrt{b_2^2+b_4^2} \end{matrix} \end{array}\right] \quad (10)$$

while $A^{(1)}(5:6,:)$ is omitted for brevity, since it is not required/involved in subsequent derivations. This is denoted as the first ET, and details are described as follows. Given $A\in\mathbb{R}^{6\times 6}$ and $\text{rank}(B)=2$, then $\mathcal{N}(B^T)$ is of dimension four and, to conform to Lemma 2, the first four columns of $M_B$ should span $\mathcal{N}(B^T)$. This result is simply obtained by solving the matrix equation $B^T\cdot\mathbf{y}_1=\mathbf{0},\ \mathbf{y}_1\in\mathbb{R}^6$, for a set of (four) orthogonal solutions, i.e., a basis of $\mathcal{N}(B^T)$. On the other hand, the last two columns of $M_B$, which span $\mathcal{R}(B)$, are constructed by solving another matrix equation $M_B(:,1:4)^T\cdot\mathbf{y}_2=0,\ \mathbf{y}_2\in\mathbb{R}^6$. Note that, since both of the above-mentioned matrix equations are at least rank deficient by two, there exist infinitely many different bases for the solution set, respectively. The result of $M_B$ in (8) is chosen because it: 1) contains many trivial entries, which simplifies the derivations afterward and 2) facilitates the generalization in Corollary 1; while there exist different methods to construct $M_B$, e.g., householder transformation [15]. Given the orthogonal $M_B$ in (8), and by the invariance of controllability/stabilizability under an ET, the pair $(A,B)$ is controllable (respectively stabilizable) iff the pair $(A^{(1)},B^{(1)})$ is controllable (respectively stabilizable), in the first transformed coordinate of the same dimension (six).

Obviously, $B^{(1)}$ is of full rank since $B^{(1)}(5:6,:)\in\mathbb{R}^{2\times 2}$ is an invertible matrix. By Lemma 2, the controllability/stabilizability analysis is equivalent to the analysis of

$$A^{(2)}=A^{(1)}(1:4,1:4)\in\mathbb{R}^{4\times 4} \quad (11)$$

and

$$B^{(2)}=A^{(1)}(1:4,5:6)\in\mathbb{R}^{4\times 2} \quad (12)$$

which is noted as the first level of DR. The next two steps mimic the previous two steps, i.e., the second ET followed by the second level of DR and, thus, briefed for compactness. Given: 1) $A^{(2)}\in\mathbb{R}^{4\times 4}$; 2) full-rank $B^{(2)}\in\mathbb{R}^{4\times 2}$; and 3) $B^{(2)}$ is already orthogonal, we perform the second ET by

$$M_{B^{(2)}}=\left[\begin{array}{cc:c} 0 & b_4/\sqrt{b_2^2+b_4^2} & \\ 0 & -b_2/\sqrt{b_2^2+b_4^2} & B^{(2)} \\ 0 & 0 & \\ 1 & 0 & \end{array}\right]\in\mathbb{R}^{4\times 4}. \quad (13)$$

In (13), $M_{B^{(2)}}(:,1:2)$ constitutes a basis of $\mathcal{N}((B^{(2)})^T)$, therefore, $M_{B^{(2)}}$ is orthogonal. In addition, in the second transformed coordinate of dimension four, we have $(A^{(3)},B^{(3)})=(M_{B^{(2)}}^T A^{(2)}M_{B^{(2)}},M_{B^{(2)}}^T B^{(2)})\in\mathbb{R}^{4\times 4}\times\mathbb{R}^{4\times 2}$, where

$$A^{(3)}(1:2,:)=\left[\begin{array}{cccc} 0 & \dfrac{-b_2\Gamma}{b_2^2+b_4^2} & 0 & \dfrac{b_4\Gamma}{b_2^2+b_4^2} \\ \sqrt{b_2^2+b_4^2} & 0 & 0 & 0 \end{array}\right] \quad (14)$$

$$(B^{(3)})^T=\left[\begin{array}{c:cc} 0_2 & \begin{matrix} 1 & 0 \\ 0 & \sqrt{b_2^2+b_4^2} \end{matrix} \end{array}\right] \quad (15)$$

while $A^{(3)}(3:4,:)$ is omitted as not required/involved in the subsequent derivations. Given the invertible $B^{(3)}(3:4,:)\in\mathbb{R}^{2\times 2}$, hence, $B^{(3)}$ is of full rank. By Lemma 2, it is equivalent to analyze the controllability/stabilizability of the pair

$$A^{(4)}=A^{(3)}(1:2,1:2)\in\mathbb{R}^{2\times 2} \quad (16)$$

and

$$B^{(4)}=A^{(3)}(1:2,3:4)\in\mathbb{R}^{2\times 2}. \quad (17)$$

This is noted as the second level of DR, to planar systems.

Therefore, if $B^{(4)}\neq 0$, or equivalently $\Gamma\neq 0$, then the pair $(A^{(4)},B^{(4)})$ is controllable, i.e., $A\in\mathcal{A}_{\mathbf{xf}}^c=\mathcal{A}_{\mathbf{xf}}^s$; otherwise $(\Gamma=0)$, $\lambda(A^{(4)})=\{0\}$, $B^{(4)}=0$, and thus $A\notin\mathcal{A}_{\mathbf{xf}}^s$, i.e., SDRE (3) is unsolvable. ■

*Remark 1: Generalization of Theorem 1.*

1) In the SDRE control system design, a solvable SDRE (3) corresponding to a selected SDC, which is a critical design issue, is commonly assumed [6], [7], [9]. This assumption (design compromise) is needed because the associated analysis was not available, even if only the preliminary controllability condition is considered [16]. Alternatively, an equivalent solvability condition is formulated in Theorem 1, which is based on the early results in WIP modeling [2] and generalized to the more challenging stabilizability analysis. The compactness of such a closed-form result is facilitated by the novel DR strategy. This strategy can also be applied to analyze more SDRE control systems, such as scout robotics [8], multiagent systems [9], and aerospace guidance [17] in the recent literature. This brief is motivated by an expectation among the control community, i.e., more theoretical support of the practical achievements of SDRE.
2) This remark indicates another direction for generalization, i.e., to analyze the feasibility of other meaningful SDC matrices. In particular, let $\bar{a}_{6i}:=\bar{a}_{6i}(\mathbf{x})\in\mathbb{R}$, $\sum_{i=1}^6\bar{a}_{6i}x_i=f_6$, and consider the set of SDC matrices

$$\bar{A}=\bar{A}(\mathbf{x})=\left[\begin{array}{c} A(1:5,:) \\ \hdashline \begin{matrix} \bar{a}_{61} & \bar{a}_{62} & \bar{a}_{63} & \bar{a}_{64} & \bar{a}_{65} & \bar{a}_{66} \end{matrix} \end{array}\right] \quad (18)$$

where $A$ is given in (7) and $\bar{A}\in\mathbb{R}^{6\times 6}$. This set of SDC matrices (18) covers all those directly/implicitly considered in [2], e.g., $A$ in (7) and later $A^*$ in (20). From a modeling perspective, the first five rows of $\bar{A}$ in (18) are exactly the same as those in the previous SDC matrix, $A$ in (7), such that certain system responses of WIP (4) are expectedly retained. On the other hand,

the flexibility on the last row can be exploited to alleviate the high gain effect caused by the yaw acceleration and/or straight-ahead velocity. This extension is formulated as Corollary 1 in the following.

*Corollary 1:* Consider $Q > 0$, $B$ in (6), and a set of generalized SDC matrices $\bar{A}$ in (18) which is parameterized by variables $\{\bar{a}_{6i}\}_{i=1}^{6}$. The three statements adopted from Theorem 1 are also equivalent.

*Proof:* For brevity, we only highlight the most significant difference with respect to the proof of Theorem 1. Considering $\bar{A}$ in (18) and $B$ in (6), at first, we adopt the ET by $M_B$ (8). As a result, $\bar{A}$ is transformed into

$$\begin{aligned}\bar{A}^{(1)} &= M_B^T \bar{A} M_B \\ &= \left[\begin{array}{c:c:c} I_3 & 0_{3\times 2} & \begin{matrix}0\\0\\0\end{matrix} \\ \hdashline & \begin{matrix}\frac{b_4}{\sqrt{b_2^2+b_4^2}} & \frac{-b_2}{\sqrt{b_2^2+b_4^2}} \\ 0 & 0 \\ \frac{b_2}{\sqrt{b_2^2+b_4^2}} & \frac{b_4}{\sqrt{b_2^2+b_4^2}}\end{matrix} & \begin{matrix}0\\1\\0\end{matrix} \\ \hdashline 0_3 & & \end{array}\right] \\ &\quad \times \left[\begin{array}{c:c} 0_3 & I_3 \\ \hdashline \begin{matrix}0 & a_2 & 0 \\ 0 & a_4 & 0\end{matrix} & 0_{2\times 3} \\ \hdashline \bar{a}_{61} \quad \bar{a}_{62} \quad \bar{a}_{63} & \bar{a}_{64} \quad \bar{a}_{65} \quad \bar{a}_{66}\end{array}\right] \cdot M_B \\ &= \left[\begin{array}{c:c} 0_3 & I_3 \\ \hdashline 0 \quad \Gamma/\sqrt{b_2^2+b_4^2} \quad 0 & \mathbf{0}_{1\times 3} \\ \hdashline * & \end{array}\right] \cdot M_B \\ &= \left[\begin{array}{c:c} A^{(2)} & B^{(2)} \\ \hdashline \multicolumn{2}{c}{\blacksquare} \end{array}\right] \in \mathbb{R}^{6\times 6}. \end{aligned} \tag{19}$$

Remarkably, the four entries $M_B(1:4,6)$ unifies/nullifies the effect by $\{\bar{a}_{6i}\}_{i=1}^{6}$, at the very beginning of derivations ($M_B^T \bar{A}$). Thus, the remaining proof is the same as the counterpart in Theorem 1, specifically, from $A^{(2)}$ in (11) and $B^{(2)}$ in (12) at the first level of DR in the proof of Theorem 1. ■

*Remark 2:* In the proof of Corollary 1, the usefulness of the selected ET by $M_B$ in (8) is again endorsed from a computational perspective. Although the design flexibility—arising from the last element ($f_6$) in the WIP dynamics (5), (18)—is of importance from a modeling perspective [2], the selected ET in (8) unifies/nullifies such a flexibility, and thus simplifies the solvability analysis regarding the considered generalization. In other words, the last row of $\bar{A}$ does not contribute to the solvability analysis. Among all SDC matrices included in this generalization, a particular example is highlighted in [2], also denoted as $A^* = A^*(\mathbf{x}) \in \mathbb{R}^{6\times 6}$ for easy comparison, that is,

$$A^* = \left[\begin{array}{c} A(1:5,:) \\ \hdashline \mathbf{0}_{1\times 3} \quad \bar{a}_{64} \quad \bar{a}_{65} \quad 0 \end{array}\right] \tag{20}$$

where $A$ is given in (7), $\bar{a}_{64} = -m_B l x_6 \mathrm{s}x_2/\eta_2$, $\bar{a}_{65} = (I_3 - I_1 - m_B l^2) x_6 \mathrm{s}(2x_2)/\eta_2$, and $\eta_2$ in (4). Such an SDC matrix $A^*$ in (20) has been shown in [2] to be more robust against high gain effect and external disturbances than $A$ in (7), through modeling analysis, simulations, and experiments.

To sum up, by virtue of the simple equivalence condition ($\Gamma \neq 0$) in Theorem/Corollary 1, the solvability of the SDRE (3) can be efficiently and offline determined. This avoids significant online computational load of examining the pointwise solvability of SDRE (as summarized in Lemma 1), with respect to $A$ in (7), $A^*$ in (20), and an extension set (18) in [2], via the *Classical SDRE* scheme. In [12, Algorithm 1], an alternative algorithm of feasible SDC constructions—with only a few steps—is given such that the applicability of the SDRE scheme is always ensured, even at those system states corresponding to unsolvable AREs (3).

### B. Solving Objective Conflict and MOI Issue

The equivalent condition in Theorem/Corollary 1 for the solvability of *Classical SDRE* scheme is further analyzed, according to the primary objective of balancing WIP without toppling [1]. Particularly, the equivalent statement $\Gamma = a_2 b_4 - a_4 b_2 = 0$ in Theorem/Corollary 1 is focused upon. Given $\{a_i, b_j\}_{i,j=2,4}$ in (5) and (6), we have $\Gamma = 0 \Leftrightarrow$

$$\begin{aligned}&(r\Gamma_1 + m_B l \mathrm{c}x_2)\big\{\big(I_2 + m_B l^2\big) m_B l x_5^2 - m_B^2 l^2 g \mathrm{c}x_2 \\ &\qquad + m_B l x_6^2 (I_2 + m_B l^2 + \Gamma_2 \mathrm{c}^2 x_2)\big\} \\ &\quad = [I_2 + m_B l (l + r\mathrm{c}x_2)] \\ &\qquad \times \big\{m_B^2 l^2 x_5^2 \mathrm{c}x_2 - \Gamma_1 m_B l g \\ &\qquad\quad + \big[m_B^2 l^2 + \Gamma_2 (m_B + 2m_W + 2J/r^2)\big] x_6^2 \mathrm{c}x_2\big\}\end{aligned} \tag{21}$$

where $\Gamma_1 = m_B + 2m_W + 2J/r^2$ and $\Gamma_2 = I_3 - I_1 - m_B l^2$. In terms of the state-space representation, (21) only depends on state variables $x_2 = \theta$, $x_5 = \dot{\theta}$, and $x_6 = \dot{\psi}$. Consider the case of balancing WIP at the upright direction ($x_2 = \theta = 0$), while the other cases of pitch angles can be derived similarly.

After calculations, (21) can be rewritten as

$$\Gamma_{I_2}\{(m_B l r) x_5^2 + [I_1 - I_3 + m_B l (r + l)] x_6^2 + m_B l g\} = 0 \tag{22}$$

$$\Gamma_{I_2} = [(m_B + 2m_W + 2J/r^2) I_2 + 2m_B l^2 (m_W + J/r^2)]/r. \tag{23}$$

Note that, among the three MOIs $\{I_i\}_{i=1}^{3}$, (22) isolates the effect by $I_2$, i.e., $I_2$ only appears in $\Gamma_{I_2}$ while $I_1$ and $I_3$ only appear in the remaining term. Since $\Gamma_{I_2}$ (23) is always positive, (22) is equivalent to

$$(m_B l r) x_5^2 + [I_1 - I_3 + m_B l (r + l)] x_6^2 + m_B l g = 0 \tag{24}$$

which is regarded as a quadratic equation of the unknown variables $x_5$ and $x_6$. Since both the constant term, $m_B l g$, and the coefficient of $x_5^2$, $m_B l r$, are always positive, (24) holds only when the coefficient of $x_6^2$ (denoted as $C_{x_6^2}$) is negative

$$C_{x_6^2} = I_1 - I_3 + m_B l (r + l) < 0. \tag{25}$$

It can be seen from (25) that the MOI configuration design of $I_1$ and $I_3$ is crucial in determining whether (25) holds, but the other MOI $I_2$ has no effect in this regard. A physical interpretation of such an MOI configuration design is illustrated by [2, Fig. 2], with more investigations from a

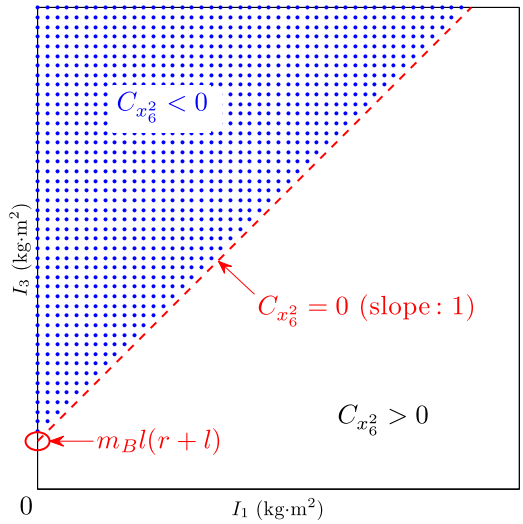


Fig. 2. $C_{x_6^2}$ corresponding to MOIs: $I_1$ and $I_3$.

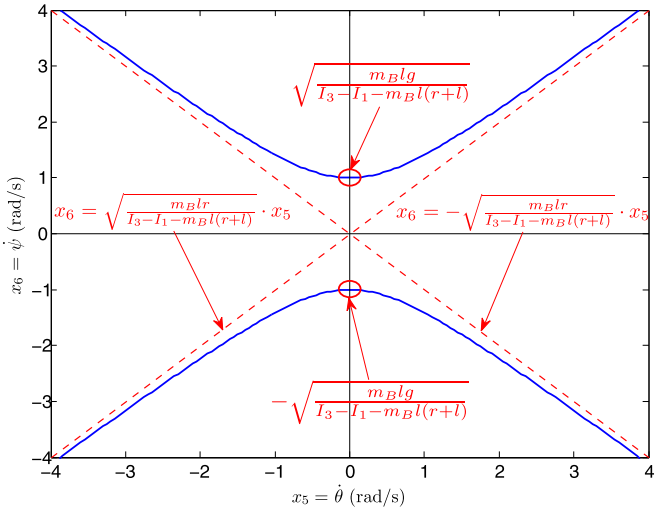


Fig. 3. Phase plane of $x_5$ and $x_6$ (when $C_{x_6^2} < 0$).

modeling perspective. For example, two MOI configurations of fat and slender WIP bodies are shown, where the latter one is generally easier to move/control and resembles the outlook of *Segway*. On the other hand, in terms of the $I_1 - I_3$ plane, Fig. 2 shows the geometric structure of (25) with three disconnected regions: the blue/dotted area corresponds to $C_{x_6^2} < 0$, the red/dashed line $C_{x_6^2} = 0$, and the other areas $C_{x_6^2} > 0$, respectively. Remarkably, the red/dashed line has slope of 1 and intersects with the $I_3-$axis at $m_B l(r+l) > 0$. In addition, in the area outside of the blue/dotted region ($C_{x_6^2} \geq 0$), by Theorem/Corollary 1 and (24), the set of SDCs (18) renders the corresponding SDRE (3) solvable, which includes SDCs $A$ in (7) and $A^*$ in (20). Regarding the blue/dotted area ($C_{x_6^2} < 0$), (24) represents a hyperbola in the phase plane of $x_5$ and $x_6$, as illustrated in the blue/solid curves in Fig 3. Its vertices and asymptotes are in the following equations, respectively

$$\left(0, \pm\sqrt{-m_B lg / C_{x_6^2}}\right) \tag{26}$$

$$x_6 = \pm\sqrt{-m_B lr / C_{x_6^2}} \cdot x_5 \tag{27}$$

where $C_{x_6^2} < 0$ by (25). According to Theorem/Corollary 1 and (24), SDRE (3) corresponding to the set of SDCs (18) is *only* unsolvable at those system states on the hyperbola. To sum up, the above-mentioned analysis is summarized as follows.

*Theorem 2:* Given $Q > 0$, $\bar{A}$ (18), $B$ (6), and the control objective of balancing the WIP pitch motion upright, the following statements, pointwise at any nonzero system state, are equivalent: 1) SDRE (3) is unsolvable; 2) $A \notin \mathcal{A}_{\mathbf{xf}}^{s\beta}$, $\beta = l, i$; and 3) $m_B lr x_5^2 + C_{x_6^2} x_6^2 + m_B lg = 0$, with $C_{x_6^2} < 0$ as given in (25) and illustrated in Figs. 2 and 3.

To conclude, regarding the control objective of upright balancing the pitch motion, the applicability of *Classical SDRE* is investigated, in terms of the solvability of the corresponding SDRE (3) with the set of SDCs (18). In particular, the dominant effect by MOI configuration design is analyzed from this computational perspective, in addition to recent modeling investigations in the literature. Specifically:

1) the MOI $I_2$ has no effect on the pointwise solvability of SDRE (3), as revealed by $\Gamma_{I_2} > 0$ in (22) and (23);
2) the other body MOIs $I_1$ and $I_3$ play dominant roles in this regard, as a result of (24) and (25). For example, the *Classical SDRE* scheme can be designed applicable everywhere in the state space, e.g., by slimming the WIP robot (decreasing the ratio $I_3/I_1$ according to [2, Fig. 2(b)]), such that the point $(I_1, I_3)$ is not in the blue/dotted region in Fig. 2. On the other hand, if the WIP configuration corresponds to $(I_1, I_3)$ located in the blue/dotted region in Fig. 2, then SDRE (3) with the set of SDCs (18) is not solvable at those system states $\{\mathbf{x} \mid \mathbf{x} \in \mathbb{R}^6$ satisfying (24)$\}$, which represents a hyperbola in the $x_5 - x_6$ phase plane (the blue/solid curves in Fig. 3). Remarkably, the SDC set (18) includes $A$ in (7) and $A^*$ in (20), both of which are presented in [2].

## IV. Simulation Validation and Analysis

The proposed WIP balancing control based on new analysis and design via the SDRE scheme is demonstrated and compared with the recent literature. The considered two control designs are: 1) the *Classical(+Alternative) SDRE* scheme adopting the SDC matrix $A$ in (7) and $A^*$ in (20), respectively. When the simulation breaks down due to unsolvable SDRE (3), as expected by $\Gamma = 0$ in Theorem/Corollary 1, the alternative scheme of feasible SDC construction is evoked [12, Algorithm 1] and 2) the *Alternative SDRE* scheme solely based on the alternative and feasible SDC construction, as a comparison to the recent literature. The focus of this demonstration is on two parts: Section IV-A illustrates the effect of MOI configurations $\{I_i\}_{i=1,3}$ on the applicability of *Classical SDRE*, with respect to the objective of upright balancing the WIP. Accordingly, an example of MOI configurations is suggested for subsequent demonstrations. Section IV-B highlights the feasibility and indispensable evocation of *Alternative SDRE*, and its potential performance advantages over *Classical SDRE*. For easy comparison, the parameter setting of WIP robot in (4) adopts the experimental setup in [2],

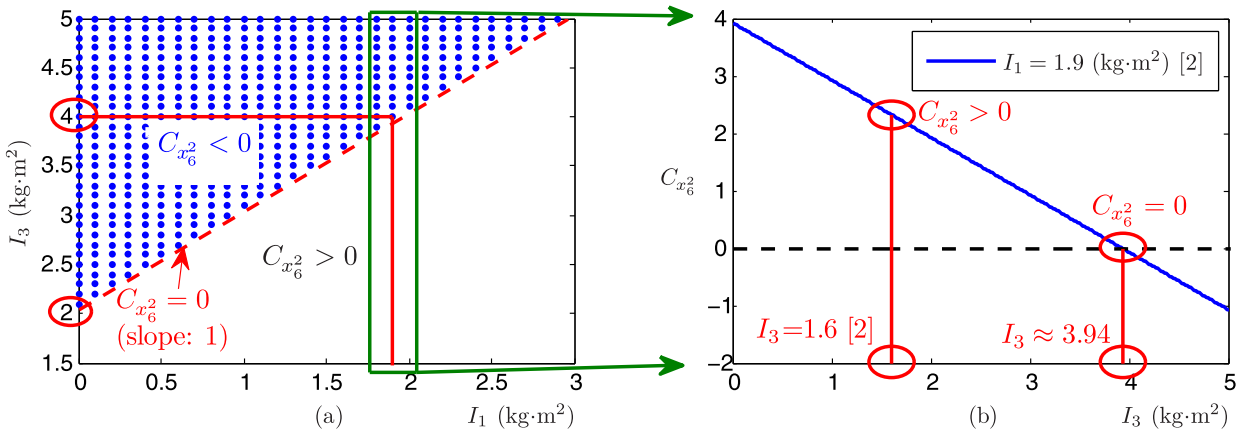


Fig. 4. $C_{x_6^2}$ corresponding to MOI setting with $I_2 = 2.1$ kg·m$^2$ [2], where (a) sign of $C_{x_6^2}$ and (b) $I_1 = 1.9$ kg·m$^2$.

except the MOI configurations $\{I_i\}_{i=1}^3$. The effect of $\{I_i\}_{i=1}^3$ will be analyzed in Section IV-A, which provides an example for Section IV-B to demonstrate its significance in affecting the applicability of *Classical SDRE*.

### A. Solvability/Feasibility of SDRE Scheme

Considering the objective of balancing the WIP at the upright direction, the MOI configuration $\{I_i\}_{i=1,3}$ is the critical factor in determining the applicability of *Classical SDRE*, according to $C_{x_6^2}$ (25) and Theorem 2. Following the experimental setup of WIP in [2], the relationship between $C_{x_6^2}$ and $\{I_i\}_{i=1,3}$ is explicitly illustrated in Fig. 4, with $I_2 = 2.1$ kg·m$^2$. Fig. 4(a) depicts three disconnected regions in terms of $C_{x_6^2}$, i.e., $C_{x_6^2} < 0$ (blue/dotted area), $C_{x_6^2} = 0$ (red/dashed line), and $C_{x_6^2} > 0$ (the others), respectively. Note that the slope of the red/dashed line is 1, which intersects the $I_3$-axis at $m_B l(r + l) = 2.04$ by (25). Fig. 4(b) focuses on the case of $I_1 = 1.9$ kg·m$^2$ [2], depicting the relationship between specific values of $C_{x_6^2}$ and $I_3$. It is worth mentioning that the case/point of $(I_1, I_3) = (1.9, 1.6)$ in [2] resides in the area of $C_{x_6^2} > 0$. This, by Theorem 2, ensures the overall solvability of corresponding SDRE (3) with respect to the set of SDCs (18), which includes $A$ in (7) and $A^*$ in (20) that are experimented/simulated in [2]. In other words, the overall applicability of *Classical SDRE* can be offline guaranteed, without need of online examination, throughout all the simulations and experiments therein.

As a step forward, we consider more cases of WIP's MOI configurations arising from, e.g., flexible loading, capacity, and component allocations. By Fig. 4(b), the critical value of $C_{x_6^2} = 0$ happens at $I_3 = 3.94$ with $I_1 = 1.9$ (kg·m$^2$). Therefore, we choose a representative example $(I_1, I_3) = (1.9, 4)$ for the following demonstrations. This point (the intersection of two red/solid lines) resides in the blue/dotted region of $C_{x_6^2} < 0$ in Fig. 4(a). According to (25) and Theorem 2, such MOI configurations render $C_{x_6^2} = -0.06$ and thus the corresponding SDREs only unsolvable at the system states $\{\mathbf{x} \in \mathbb{R}^6 \mid 1.22x_5^2 - 0.06x_6^2 + 59.53 = 0\}$, with respect to the set of classical SDCs (18). The geometric structure of these unsolvability states is a hyperbola in the $x_5 - x_6$ phase plane, as depicted/analyzed in Fig. 3, and more details considering this simulation setup will be given in Section IV-B as follows.

### B. Performance of Classical and Alternative SDREs

Assume a challenging scenario with a high initial yaw rate as compared to the experiments/simulations in [2], i.e., $x_6(0) = \dot{\psi}(0) = 480$ rad/s, while the other state variables start from zero. Let $R = I_2$ and $Q = \text{diag}(10^{-6}, 10^{-2}, 10^{-6}, 10^{-6}, 10^{-6}, 3.3 \times 10^{-2})$ for both *Classical* and *Alternative SDREs*, which reveals several performance advantages of the latter. The weights on $(x_2, x_6) = (\theta, \dot{\psi})$ and $\mathbf{u} = (T_L, T_R)^T$ are higher than the other variables because the WIP balance control of $\theta$ is the main objective in this brief and most literature [1], while regulating the yaw rate $(\dot{\psi})$ and accounting for the motor/actuator constraint on $(T_L, T_R)$.

In Fig. 5, the performances to regulate the WIP's yaw motion while keeping its balance, via both the *Classical* and *Alternative SDRE* schemes, are demonstrated. Regarding *Classical SDRE*, the performances by SDCs $A$ in (7) and $A^*$ in (20) differ insignificantly. Hence, the following results focus on the comparison between classical SDC (20) and the alternative SDC construction scheme. It should be emphasized first that the red/vertical lines shown in Fig. 5(a)–(f) indicate the breakdown instant via *Classical SDRE*, at $t \approx 17.769$ s; whereas there is no breakdown via *Alternative SDRE* throughout the simulation, as expected. According to Theorem/Corollary 1, the breakdown due to the unsolvable SDRE (3) can be determined by the condition $\Gamma = 0$, which is depicted in Fig. 5(e) with its close-up in Fig. 5(f). Regarding the control objective to regulate $\theta = 0$ in Fig. 5(a), the condition can be further analyzed by virtue of Theorem 2. Given the analysis in Section IV-A, the corresponding SDREs are only unsolvable at $\{\mathbf{x} \in \mathbb{R}^6 \mid 1.22x_5^2 - 0.06x_6^2 + 59.53 = 0\}$ with respect to the classical SDC (20), which is explicitly illustrated in the $x_5 - x_6$ phase portrait in Fig. 5(g) and its close-up in Fig. 5(h). These unsolvability states constitute a hyperbola, as depicted by the red/solid curves, which has vertices at $(0, \pm 30.29)$ by (26) and asymptotes $x_6 = \pm 4.33x_5$ by (27). As the WIP's yaw rotation slows down ($\dot{\psi}$ decreasing, black/dashed line), *inevitably*, the system/yaw trajectory crosses the hyperbola where *Classical SDRE* fails. This needs careful attention

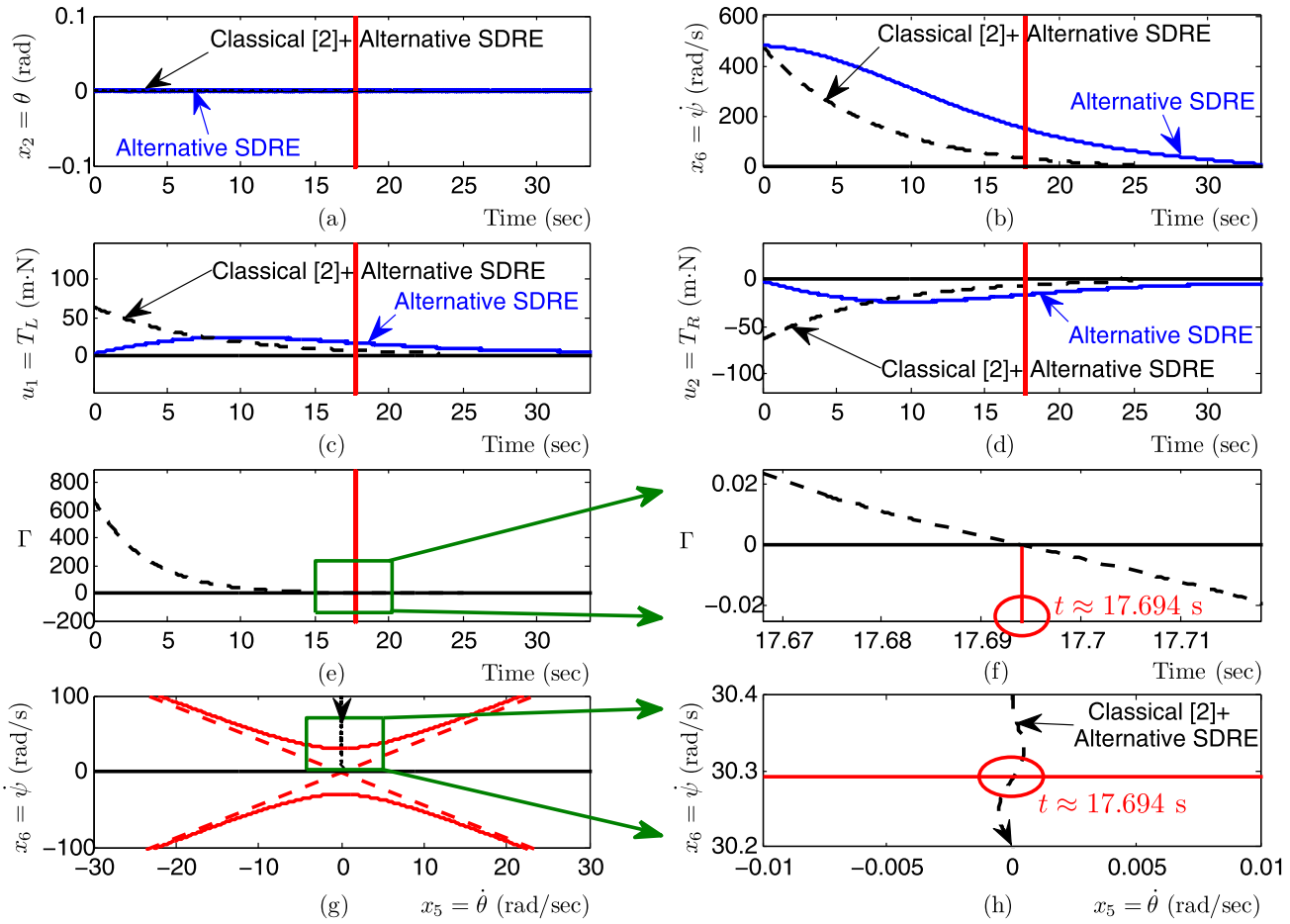


Fig. 5. (a) Time history of $\theta$. (b) Time history of $\dot{\psi}$. (c) Control input $T_L$. (d) Control input $T_R$. (e) Time history of the parameter $\Gamma$. (f) Zoomed time history of the parameter $\Gamma$. (g) $x_5 - x_6$ phase plane with (h) zoomed $x_5 - x_6$ phase plane, via classical [2] and alternative SDREs.

because the trajectory planning is crucial in control system designs but can be readily resolved by *Alternative SDRE*.

When *Classical SDRE* breaks, the controller computations can still be continued successfully by resorting to the alternative construction of feasible SDCs. In Fig. 5(a)–(d), the black/dashed lines represent the results of *Classical + Alternative SDRE*, and the blue/solid lines are the results solely by *Alternative SDRE*. However, in this simulation setup, the *Classical + Alternative SDRE* scheme is still less preferred with respect to the control effort. As revealed by Fig. 5(c) and (d) together with the numerical results in the end of this paragraph, the *Alternative SDRE* [12] outperforms the other in this setting. Regarding *Classical + Alternative SDRE*, the alternative scheme is evoked only at the time instant ($t \approx 17.769$) and, thus, does not contribute to the overall energy ($\int_t ||\mathbf{u}(t)||^2$). At the instant, as shown in Fig. 5(c) and (d), the instantaneous absolute control effort $(u_1, u_2)$ is less than the overall maximum, which is required by *Classical SDRE* at the very beginning. Quantitatively, the following summarize numerics on various performance criteria between *Alternative* and *Classical SDREs*. With respect to $\mathbf{u} = [u_1, u_2]^T = [T_L, T_R]^T$ (m · N), *Alternative SDRE* requires at most 23.8 m·N for each control input/wheel torque ($\sup_{t,i} |u_i(t)|$), whereas 64.2 m·N via the other scheme. In addition, the total maximum torque ($\sup_t ||\mathbf{u}(t)||$) is 33.5 m·N for *Alternative SDRE*, which is still better than the other (90.8 m·N). Moreover, *Alternative SDRE* consumes less than half of the overall energy ($\int_t ||\mathbf{u}(t)||^2$) than the other, i.e., $1.5 \times 10^4$ as opposed to $3.1 \times 10^4$. Notably, all the control torques via *Alternative SDRE* are within the physical constraint, which is (at least) 33 m·N according to the experiments in [2].

From an implementation perspective, since the computation precision varies across different platforms/hardware, it is suggested to introduce a switching threshold, from *Classical SDRE* to *Alternative SDRE*, corresponding to Theorem/Corollary 1, Fig. 5(e) and (f). Specifically, within the region $\Gamma \leq \epsilon$, where $\epsilon \in \mathbb{R}_{>0}$ denotes the threshold, the SDRE scheme is switched to *Alternative SDRE*. Note that the threshold $\epsilon$ is preferably as conservative as necessary, such that no breakdown ever occurs. An example can be inferred from Fig. 5(f), where $\Gamma^* := \inf_t |\Gamma(t)| \approx 10^{-4}$ among all simulation time instants, and the width $\epsilon \geq \Gamma^*$ is suggested. A similar consideration applies to the design of MOI configurations corresponding to Theorem 2, Figs. 4 and 5(g) and (h). On the other hand, the overall applicability via both *Alternative SDRE* and *Classical + Alternative SDRE*, in terms of the ARE's solvability, has been offline and efficiently ensured by the analy-

sis in Section III. Regarding *Classical(+Alternative) SDRE*, the proposed results can enhance its computational performance, since the associated intensive computations to online check the ARE's solvability has been substantially alleviated by the reduced-dimensional equivalence condition, even at those system states corresponding to unsolvability.

## V. Conclusion

This brief presents a new SDRE control analysis and design for the WIP robot. Early literature focuses on the control design from a modeling aspect, demonstrating the advantages of SDRE over other techniques. Progressively, we analyze the scheme from a computational perspective. The results highlight a unified compact equivalence condition with reduced dimensionality on the solvability of AREs, corresponding to all the meaningful SDCs from the early modeling findings. Significance includes: 1) any (un)expected implementation breakdown is analytically precluded, or resolved by an alternative SDC construction. This is quite valued as *safety* is always the main concern (with respect to a commercialized WIP product *Segway*) and 2) the computational performance is improved by avoiding the excessive online solvability examination of AREs, pointwise at each time instant. This benefits the design toward a more agile, lower-cost, and thus more competitive product. Notably, the novel design strategy can be extended to analytically support more SDRE applications, responding to a recent interest in the community, i.e., enhancing the computational capability via SDRE. Moreover, potentials of the alternative SDRE scheme are demonstrated in simulations, encouraging further analysis in the SDRE control performance.

## References


[1] R. P. M. Chan, K. A. Stol, and C. R. Halkyard, "Review of modelling and control of two-wheeled robots," *Annu. Rev. Control*, vol. 37, no. 1, pp. 89–103, Apr. 2013.

[2] S. Kim and S. J. Kwon, "Nonlinear optimal control design for underactuated two-wheeled inverted pendulum mobile platform," *IEEE/ASME Trans. Mechatron.*, vol. 22, no. 6, pp. 2803–2808, Dec. 2017.

[3] S. Delgado and P. Kotyczka, "Energy shaping for position and speed control of a wheeled inverted pendulum in reduced space," *Automatica*, vol. 74, pp. 222–229, Dec. 2016.

[4] J. Huang, S. Ri, L. Liu, Y. Wang, J. Kim, and G. Pak, "Nonlinear disturbance observer-based dynamic surface control of mobile wheeled inverted pendulum," *IEEE Trans. Control Syst. Technol.*, vol. 23, no. 6, pp. 2400–2407, Nov. 2015.

[5] K. Yokoyama and M. Takahashi, "Dynamics-based nonlinear acceleration control with energy shaping for a mobile inverted pendulum with a slider mechanism," *IEEE Trans. Control Syst. Technol.*, vol. 24, no. 1, pp. 40–55, Jan. 2016.

[6] T. Çimen, "Survey of state-dependent Riccati equation in nonlinear optimal feedback control synthesis," *J. Guid. Control Dyn.*, vol. 35, no. 4, pp. 1025–1047, Aug. 2012.

[7] J. R. Cloutier and C. N. D'Souza, and C. P. Mracek, "Nonlinear regulation and nonlinear $H_\infty$ control via the state-dependent Riccati equation technique: Part 1, theory; part 2, examples," in *Proc. Internat. Conf. Nonlinear Probl. Aviation Aerosp.*, Aug. 1996, pp. 117–141.

[8] A. H. Korayem, S. R. Nekoo, and M. H. Korayem, "Sliding mode control design based on the state-dependent Riccati equation: Theoretical and experimental implementation," *Int. J. Control*, to be published. doi: 10.1080/00207179.2018.1428769.

[9] M. H. Korayem and S. R. Nekoo, "Controller design of cooperative manipulators using state-dependent Riccati equation," *Robotica*, vol. 36, no. 4, pp. 484–515, Apr. 2018.

[10] Y. Batmani, M. Davoodi, and N. Meskin, "Nonlinear suboptimal tracking controller design using state-dependent Riccati equation technique," *IEEE Trans. Control Syst. Technol.*, vol. 25, no. 5, pp. 1833–1839, Sep. 2017.

[11] K. D. Hammett, C. D. Hall, and D. B. Ridgely, "Controllability issues in nonlinear state-dependent Riccati equation control," *J. Guid. Control Dyn.*, vol. 21, no. 5, pp. 767–773, Oct. 1998.

[12] L.-G. Lin, J. Vandewalle, and Y.-W. Liang, "Analytical representation of the state-dependent coefficients in the SDRE/SDDRE scheme for multivariable systems," *Automatica*, vol. 59, pp. 106–111, Sep. 2015.

[13] K. Zhou, J. C. Doyle, and K. Glover, *Robust Optimzation Control*. Upper Saddle River, NJ, USA: Prentice Hall, 1996.

[14] X. Liu, X. Xin, Z. Li, and Z. Chen, "Near optimal control based on the tensor-product technique," *IEEE Trans. Circuits Syst. II, Express Briefs*, vol. 64, no. 5, pp. 560–564, May 2017.

[15] C.-T. Chen, *Linear System Theory and Design*, 2nd ed. New York, NY, USA: Holt, Rinehart Winston, 1984.

[16] F. Topputo, M. Miani, and F. Bernelli-Zazzera, "Optimal selection of the coefficient matrix in state-dependent control methods," *J. Guid. Control Dyn.*, vol. 38, no. 5, pp. 861–873, Sep. 2015.

[17] L.-G. Lin and M. Xin, "Missile guidance law based on new analysis and design of SDRE scheme," *J. Guid. Control Dyn.*, to be published. doi: 10.2514/1.G003544.